

## Supporting Information

### Strategy to Boost Catalytic Activity of Polymeric Carbon Nitride: Synergistic Effect of Controllable in situ Surface Engineering and Morphology

Yuan-Yuan Li<sup>1</sup>, Yuan Si<sup>1</sup>, Bing-Xin Zhou<sup>1</sup>, Wei-Qing Huang<sup>1,#</sup>, Wangyu Hu<sup>2</sup>, Anlian Pan<sup>2</sup>, Xiaoxing Fan<sup>3</sup>, Gui-Fang Huang<sup>1,\*</sup>

1. Department of Applied Physics, School of Physics and Electronics, Hunan University, Changsha 410082, China

2 School of Materials Science and Engineering, Hunan University, Changsha 410082, China

3. School of Physics, Liaoning University, Shenyang, 110036. P. R. China

### Experimental Section

All the chemicals were analytical grade reagents and used directly without any further purification.

**Synthesis of Bulk CN:** Bulk CN was prepared by a thermal polymerization method. Typically, 1 g melamine was placed into a 50 mL ceramic crucible with a cover. Then the crucible was heated to 550 °C at a heating rate of about 5 °C min<sup>-1</sup> for 2 h in a muffle furnace. Finally, the crucible was cooled naturally to room temperature and CN powders with canary yellow color were obtained.

**Formation of CM Complexes:** The CM complexes were prepared by mixing melamine and cyanuric acid in 80 mL of DI water in a beaker under an oil bath for 4h. Finally, the beaker was cooled naturally to room temperature and white CM powders were obtained. The CM complexes formed by using 1g melamine and 1g cyanuric acid at different oilbath temperatures(100, 120 and 140 °C) were labelled as CM<sub>100</sub>, CM<sub>120</sub> and CM<sub>140</sub>, respectively. The CM complexes obtained at fixed oil bath temperature of 120°C with different ratios of cyanuric acid and melamine (0.5:1, 1:1 and 1.5:1) were named as CM-0.5, CM-1.0 and CM-1.5, respectively.

**Synthesis of CN-s:** A very similar procedure to CN was conducted to synthesize CN-s. The only difference was that CM powders were used as precursor for thermal polymerization. The CN-s derived from CM<sub>100</sub>, CM<sub>120</sub> and CM<sub>140</sub>, CM-0.5, CM-1.0 and CM-1.5 were denoted as CN-s-100, CN-s-120, CN-s-140, CN-s-0.5, CN-s-1.0 and CN-s-1.5, respectively. The products obtained by calcination CM-1.0 powders for 2, 3 and 4 hours were denoted as CN-s-1.0-2h, CN-s-1.0-3h and CN-s-1.0-4h, respectively.

**Characterizations:** The morphologies of samples were characterized by the scanning electron

microscopy (SEM) (Hitachi S-4800). Transmission electron microscopy (TEM) images were observed on the Hitachi H600 with 200 kV acceleration voltage. Powder X-ray diffraction (XRD) analysis were performed by a PANalytical X'pert diffractometer operated at 40 kV and 40 mA using Cu K $\alpha$  radiation. X-ray photoelectron spectroscopy (XPS) was carried out using a Thermo Scientific Escalab 250Xi spectrometer and Fourier transform infrared (FTIR) spectra were recorded on a Thermo Nicolet 6700 spectrometer. UV-vis spectroscopy was measured on a Shimadzu UV-2600 spectrophotometer. Nitrogen adsorption/desorption measurement was performed at -196 °C using a Micromeritics instrument (3Flex Version 3.01). Classic relative pressure range ( $P/P_0 = 0.05-0.20$ ) was chosen to determine the specific BET surface area. Photoluminescence (PL) spectra were recorded on a Hitachi F-7000 fluorescence spectrometer.

Photoelectrochemical measurement: The photoelectrochemical measurements were performed using a standard three-electrode system on a CHI 660E electrochemical station. An Ag/AgCl and a Pt plate were used as the reference and counter electrode, respectively. And an aqueous solution containing 0.5 M Na<sub>2</sub>SO<sub>4</sub> (PH=7) was used as the electrolyte. 5 mg photocatalysts were loaded on the surface of FTO glass (1 cm  $\times$  2 cm) evenly, which was chosen as the working electrode. In this experiment, a 55 W filament lamp was used as the visible light source. The applied potential was converted into the RHE scale using the Nernst equation;  $E_{RHE} = E_{Ag/AgCl} + 0.059 \times PH + 0.197$ . The Mott-Schottky plots were recorded at an AC voltage magnitude of 7 mV with the frequency of 1000, 3000 and 5000Hz. Electrochemical impedance spectroscopy (EIS) was carried out in the frequency range of 0.01 Hz and 1000 kHz. The photocurrent response of the photocatalysts as light on and off was measured without bias voltage.

Evaluation of Photocatalytic Activity: Photocatalytic H<sub>2</sub> evolution activities were evaluated in a closed system equipped with a pressure detector to examine the pressure of the evolved gases during photocatalytic reactions. In a typical experiment of water splitting for hydrogen evolution, photocatalyst (50 mg) and methanol (33 mL) serving as the sacrificial electron donor were added to ultrapure water (300 mL) under stirring. Then, H<sub>2</sub>PtCl<sub>6</sub> aqueous solution was added as the precursor for the co-catalyst Pt, which was in-situ photoreduced during the photocatalytic reaction (~1 wt% Pt). Finally, the sealed quartz tube was side-irradiated under visible light by using a 300 W xenon lamp equipped with a 420 nm cutoff filter with 57 mWcm<sup>-2</sup>. The reaction temperature was carefully

maintained at room temperature. During the visible light irradiation, the evolved gas was collected at the given time intervals and analyzed with Shimadzu gas chromatography equipped with a thermal conductive detector (TCD) having high-purity Ar carrier gas.

**The photoelectrocatalytic OER Activity:** The OER experiment was performed on an electrochemical work station (CHI 660E) with a three-electrode setup and a salt bridge in 1.0 M KOH (PH=14) solution. A graphite rod was used as the counter electrode, and Ag/AgCl electrode with a salt bridge served as the reference electrode. 1.5 mg photocatalyst loaded on nickel foam (NF) glass (1 cm × 1 cm) was chosen as the working electrode. Linear sweep voltammetry (LSV) was conducted with a scan rate of 20 mV s<sup>-1</sup>. The recorded potentials were converted using the equation:  $E(\text{RHE}) = E(\text{Ag/AgCl}) + 0.197 + 0.059 \times \text{pH}$ .

**The turn over frequency (TOF) calculated:** The electrode activity or the intrinsic activity of each active site is expressed by TOF. The TOF requires the unit active component (the equivalent of Pt amount), when the sample is as photocatalyst.<sup>1, 2</sup> Therefore, the TOF value was calculated from the equation as follow:

$$\text{TOF} = n_{\text{hydrogen}} / 2n_{\text{Pt}}t$$

In the equation,  $n_{\text{hydrogen}}$  is the total mole amounts of H<sub>2</sub> molecules after reaction,  $n_{\text{Pt}}$  is mole amounts of atoms and  $t$  is the reaction time.

**Photodegradation Activity:** Photodegradation of rhodamine (RhB) over samples was performed through a reactor with a volume of about 100 mL. Typically, 10 mg samples were dispersed in the reactor with 80 mL RhB solution (10 mg L<sup>-1</sup>). After the adsorption-desorption equilibrium, the solution was illuminated using a 55 W filament lamp as the light resource. The concentration of RhB solution was measured using UV-vis spectroscopy (UV-5100, Anhui Wanyi). The degradation ratio ( $\beta$ ) of RhB over samples is calculated:

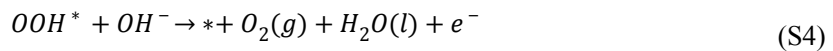
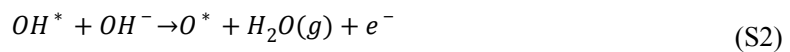
$$\beta = (1 - C_t/C_0) \times 100\% = (1 - A_t/A_0) \times 100\% \quad (1)$$

Where  $C_0$  is the primeval concentration of organic pollutants,  $C_t$  is the concentration after degrading.  $A_0$  and  $A_t$  are the relevant absorbance values.

**Methods and Models:** All our calculations are based on density functional theory (DFT) in conjunction with the projector-augmented-wave (PAW) potential as implemented by the Vienna ab

initio simulation package (VASP).<sup>3, 4</sup> The Perdew–Burke–Ernzerhof generalized gradient approximation (GGA) with the approach of DFT-D3 correction is adopted to correct the weak van der Waals-like interactions.<sup>5, 6</sup> The cutoff energy for the plane-wave basis set is 500 eV. Geometry optimization is carried out before single point energy calculation and the force on the atoms is less than 0.01 eV/Å. the first Brillouin zone is sampled with a Monkhorst–Pack grid of  $5 \times 5 \times 1$ . All atomic positions were fully relaxed until the force is less than 0.01 eV/Å. We set the criterion for the total energy to be  $1.0 \times 10^{-6}$  eV. A vacuum space of 15 Å along the z direction is used to avoid artificial interaction. We employed  $2 \times 2$  g-C<sub>3</sub>N<sub>4</sub> supercell as calculation model. After optimization, the lattice constant of this supercell is 14.24 Å, which could avoid the interaction between the adsorbed molecules. This calculation model is widespread used in the work on g-C<sub>3</sub>N<sub>4</sub>.<sup>7, 8</sup> Due to the -OH groups on CN-s surface is confirmed in experiment, we add two OH molecules on the supercell g-C<sub>3</sub>N<sub>4</sub> as corresponding calculation model.

In alkaline media, the four electron OER pathway could be summarized by the following steps



where \* stands for an active site on the graphene surface, (l) and (g) refer to gas and liquid phases, respectively, and O\*, OH\* and OOH\* are adsorbed intermediates. The detailed calculations for the free energy diagram of OER reaction were followed the approach of Nøeskov et al.<sup>9, 10</sup>

We calculate five different configuration of two hydroxyl adsorption. The structures and energies of these configurations are shown in Figure S12 and Table S5, respectively. The most stable configuration (I) CN-s is used to evaluate the activity of OER in manuscript. Meanwhile, we have examined the free energy diagram of configuration III CN-s (Its stability is second only to configuration I.), as shown in Figure S13. The overpotential of configuration III CN-s (1.68 eV) is similar to the configuration I (1.66 eV), while the rds (rate-determining-step) is transfer from second

step to first step after two hydroxyl groups adsorption with configuration III. Therefore, the different locations of two hydroxyl groups does not change the existing conclusion.

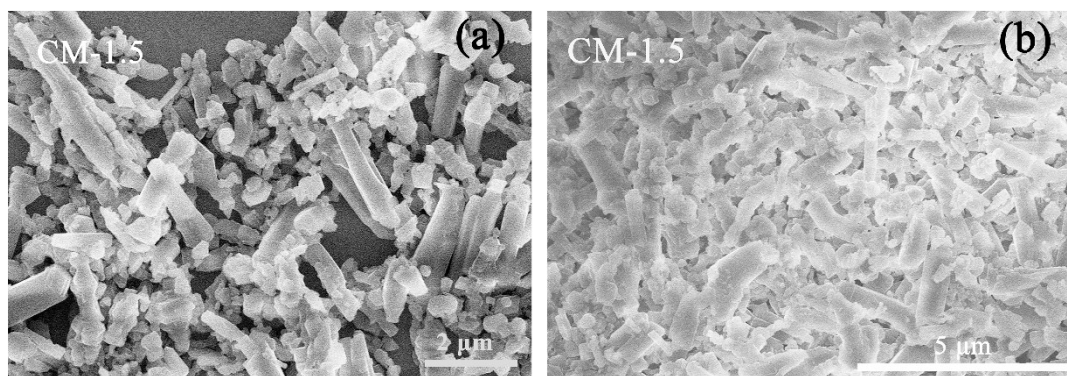


**Fig. S1.** SEM images of a, b) CM-1.5

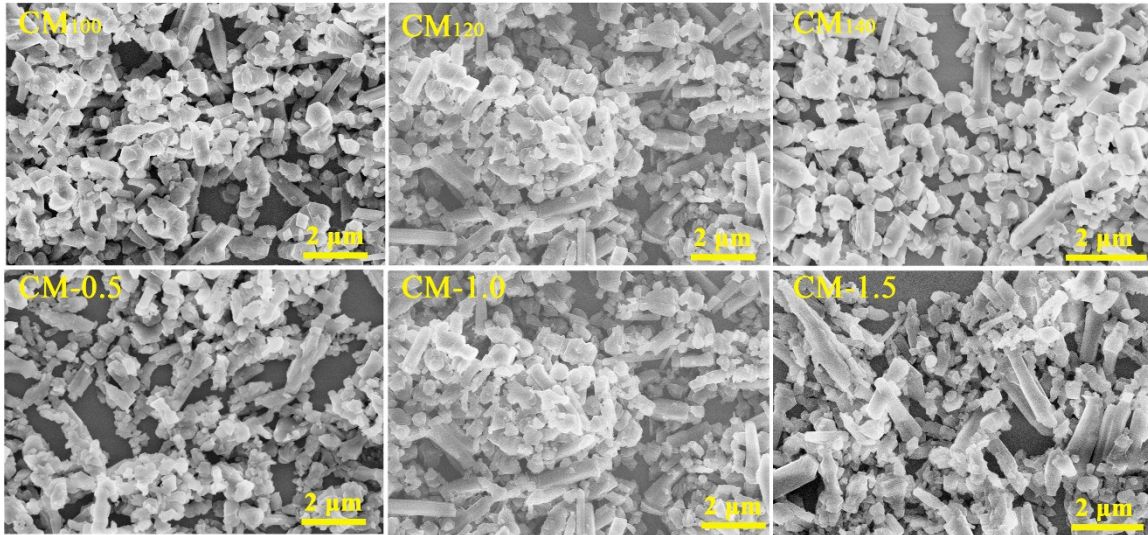


**Fig. S2.** SEM images of a) CM<sub>100</sub>, b) CM<sub>120</sub>, c) CM<sub>140</sub>, d) CM-0.5, e) CM-1.0 and f) CM-1.5.

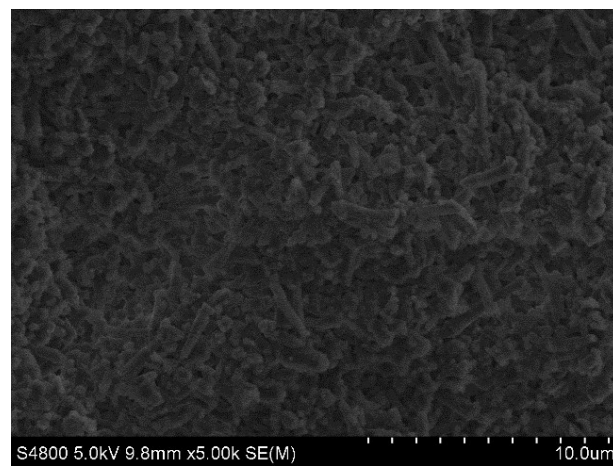


**Fig. S3.** SEM images of CM-1.0.

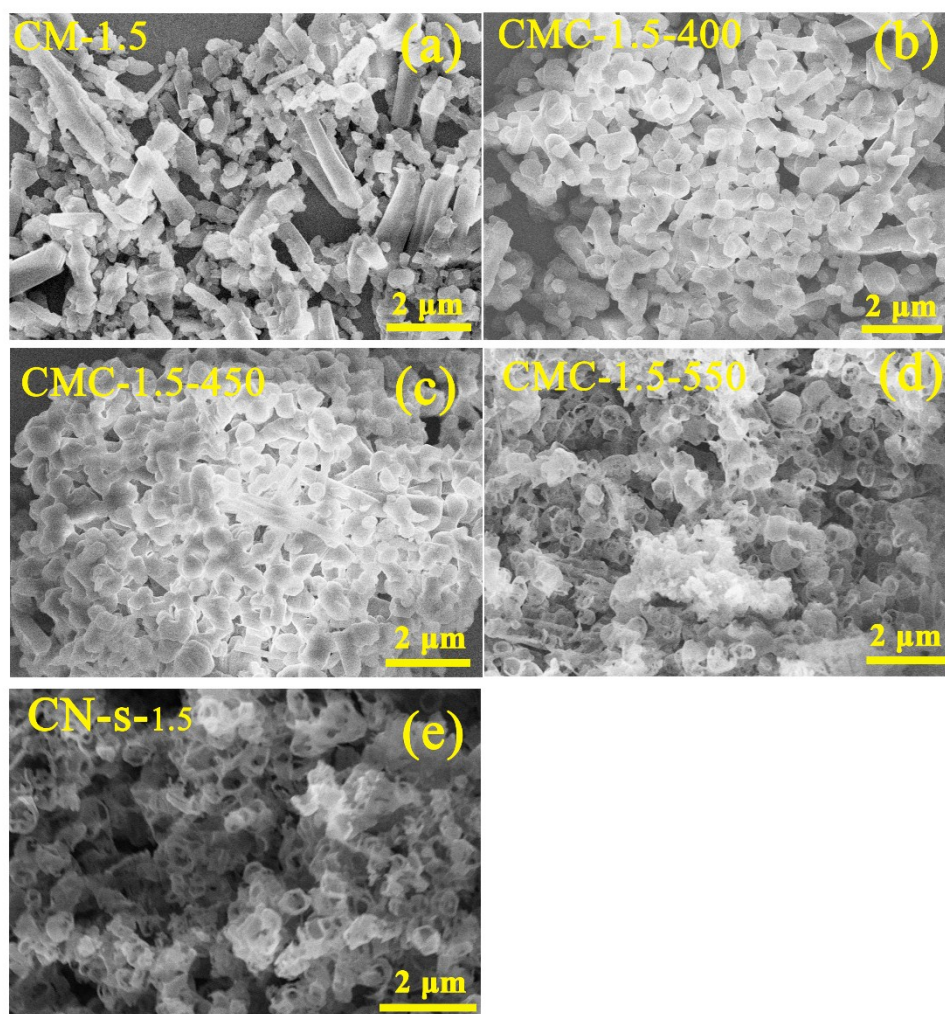


**Fig. S4.** SEM images of a) CM-1.5, b) CMC-1.5-400, c) CMC-1.5-450, d) CMC-1.0-550 and e) CN-s-1.5. The CM precursor shows a non-uniform mixed rod-like and spherical structure. Interestingly, the mixed rod-like and spherical CM precursor gradually change into uniform spherical structure up to 400 °C via an in situ etching-intralayered Ostwald ripening process. As the temperature further increases to 550 °C, the thermal etching is initiated at the center of the spherical precursor with increasing temperature, thus producing the hollow hydroxyl-rich CN hemispherical nanoshells, which become more uniform with annealing time.

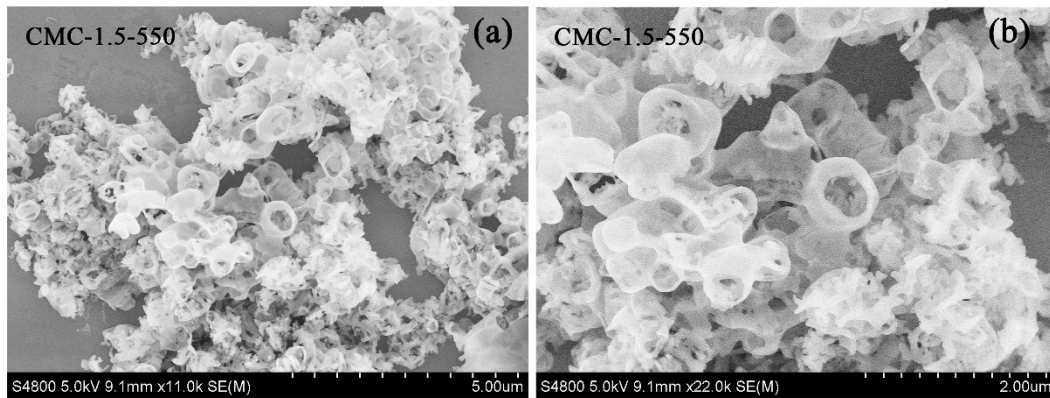


**Fig. S5.** SEM images of a, b) CMC-1.5-550.

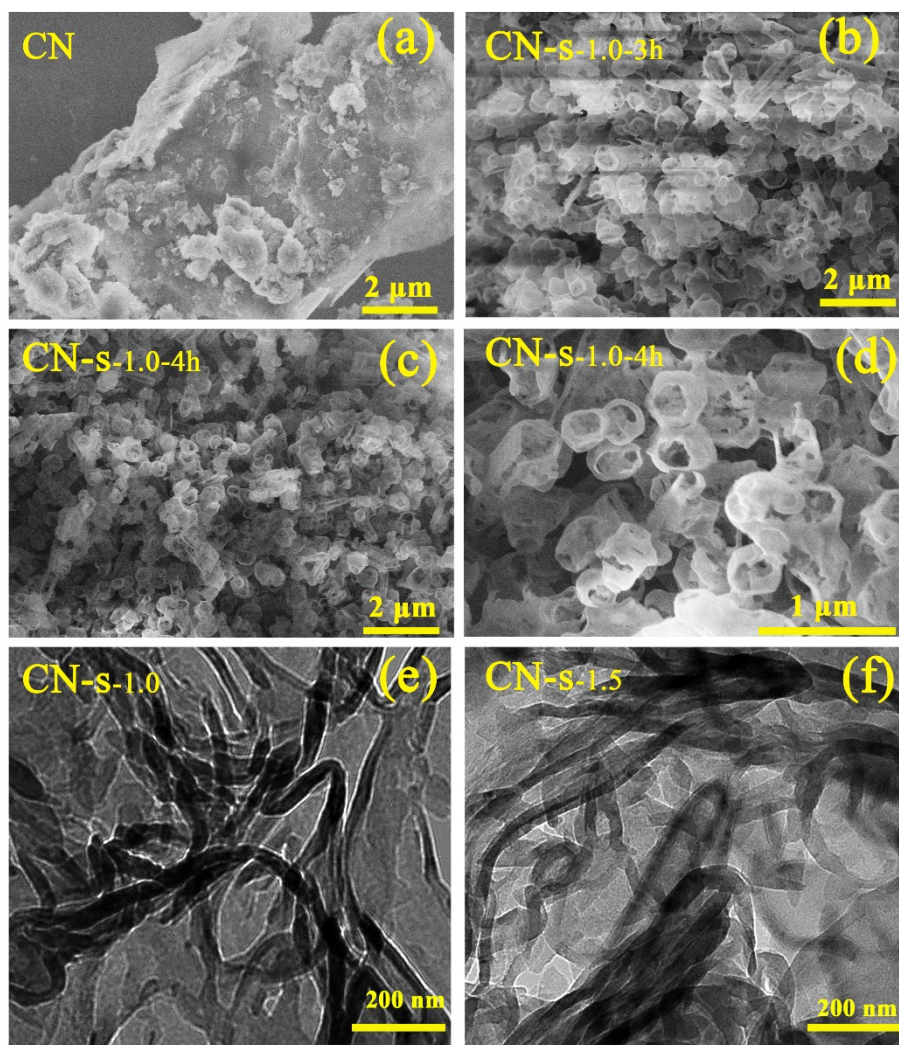


**Fig. S6.** SEM images of a) CN, b) CN-s-1.5-3h and c, d) CN-s-1.5-4h. TEM of e) CN-s-1.0 and f) CN-s-1.5.

**Table S1.** Comparison of BET surface areas of CN-s-1.5 and CN photocatalyst with other CN-based catalysts.

Photocatalyst	materials	Calcining temperature (and time)	BET surface areas (m <sup>2</sup> g <sup>-1</sup> )	Ref.
CN	melamine	550 °C (2h)	10.88	This work
CN-s-1.5	melamine, cyanuric acid	550 °C (2h)	92.83	
CN	melamine	550 °C (2h)	6.5	11
Hollow CN	melamine, cyanuric acid	550 °C (2h)	45	12
CN	Melamine	500 °C (4h)	3.73	13
P-doped CN tubes	Melamine, cyanuric acid, phosphoric acid	500 °C (4h)	22.95	
CN	Melamine	500 °C (4h)	14	14
horn-like hollow CN tube	Melamine, ammonium bromide	500 °C (4h)	58.2	
CN	Melamine	550 °C (4h)	15	15
S doped CN porous rods	Melamine, tri- thiocyanuric acid	550 °C (4h)	37	

CN	Melamine	550 °C (4h)	11.3	16
CN nanosheets	Melamine, dicyandiami de	550 °C (3h)	37	17
CN	Melamine	550 °C (3h)	12	18
CN nanosheets	Melamine, 1,4- dihydroxy- 2,5- benzoquino ne	550 °C (3h)	80	
CN	Melamine	550 °C (4h)	8.2	19
O-doped porousCN nanosheets	Melamine, hydrogen peroxide		36.3	

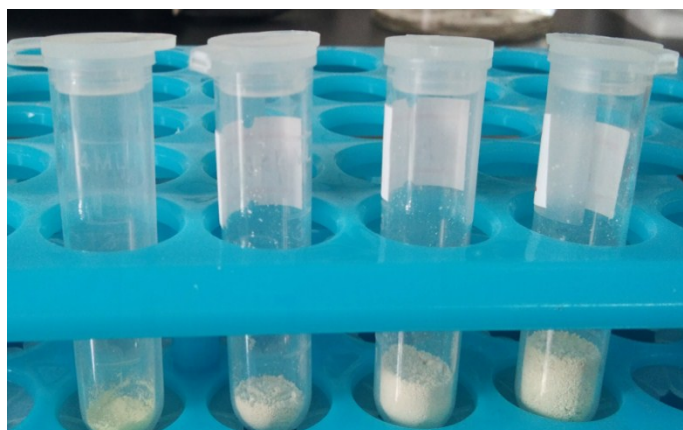


**Fig. S7.** Pictures of 50 mg CN, CN-s-0.5, CN-s-1.0 and CN-s-1.5. (The order goes from left to right.)



**Fig. S8.** Pictures of 50 mg CN, CN-s-1.0-2h, CN-s-1.0-3h and CN-s-1.0-4h. (The order goes from left to right.)

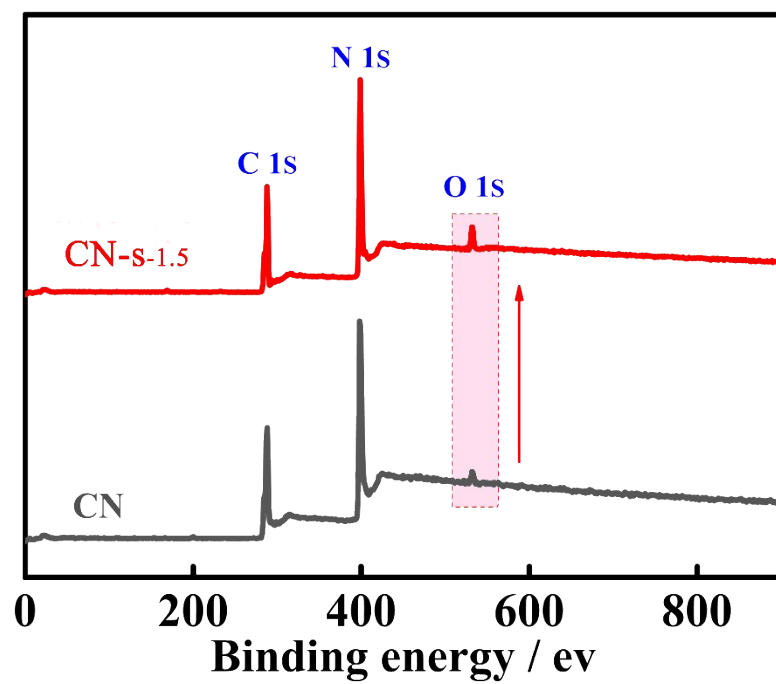
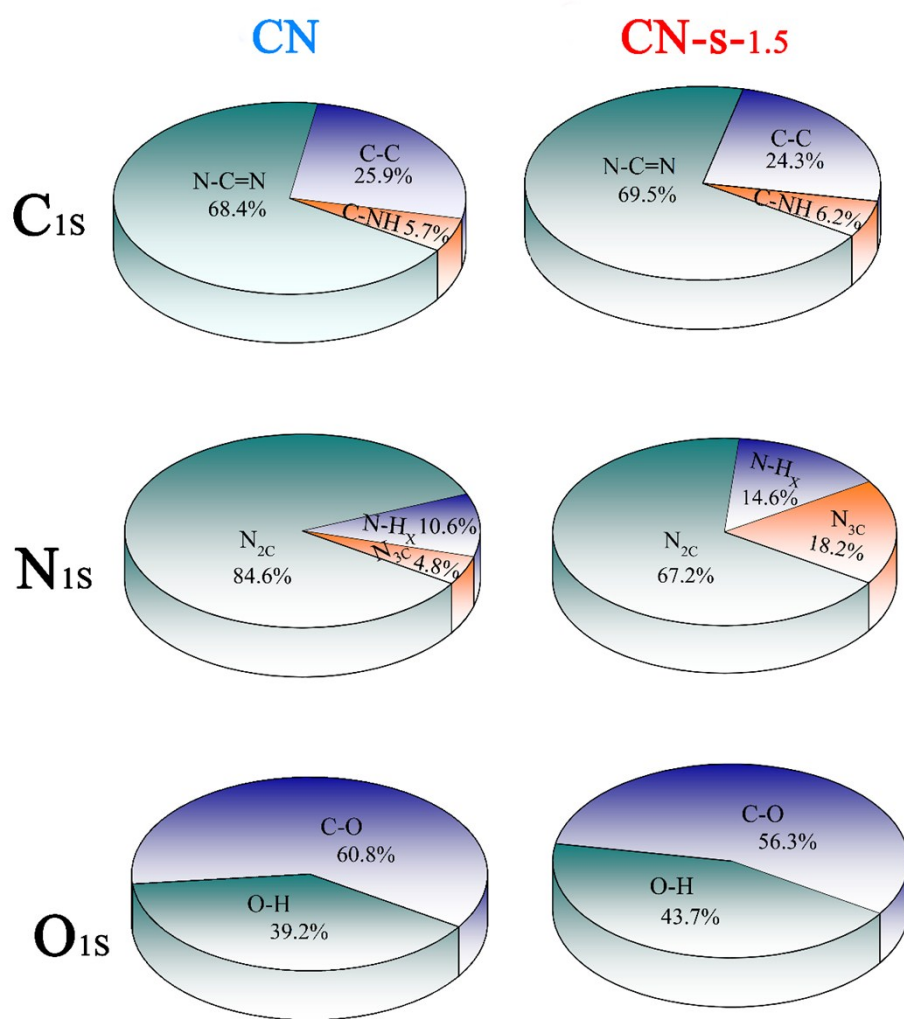


Fig. S9. XPS survey spectra of CN and CN-s-1.5.



**Fig. S10.** Summarized XPS data for the components ratios of C<sub>1s</sub>, N<sub>1s</sub>, and O<sub>1s</sub> for CN and CN-s-1.5.

**Table S2.** Summarized XPS data for CN and CN-s-1.5 surface C, N and O atom ratios determined from quantitative analyses are provided.

XPS			
samples	C	N	O
CN	42.5%	54.6%	2.9%
CN-s-1.5	39.7%	57.1%	5.1%

**Table S3.** Summarized XPS data for CN and CN-s-1.5 surface N/C atom ratios determined from quantitative analyses are provided.

XPS	
samples	N/C
CN	1.28
CN-s-1.5	1.39

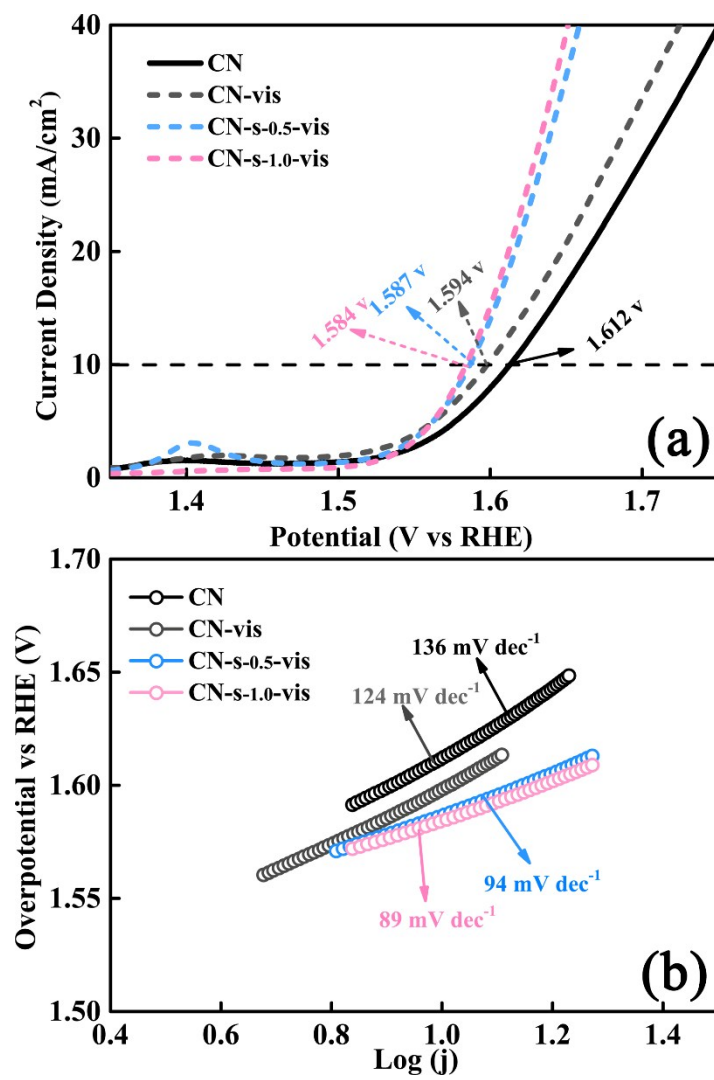


**Fig. S11.** a) Linear sweep voltammetry curves and b) Tafel plots of CN, CN-vis, CN-s-0.5-vis, and CN-s-1.0-vis.

**Table S4.** The OER catalytic activities of the prepared CN-s-1.5 and commercial RuO<sub>2</sub> catalyst.

Catalyst (Electrolyte)	Overpotential mV (vs. RHE)	Tafel plots (mVdec <sup>-1</sup> )	Reference
CN-s-1.5 (NF 1.0M KOH)	330 (55 W filament lamp)	87	This work
RuO <sub>2</sub> (PC 1.0M KOH)	400	78	<i>Nat. Commun.</i> , 44 (2018) 181-190.
RuO <sub>2</sub> (PC 1.0M KOH)	>330	76	<i>Nano Energy</i> 61 (2019) 576-583.
RuO <sub>2</sub> (PC 0.1M KOH)	320	-	<i>ACS Energy Lett.</i> , 2 (2017) 876-881.
RuO <sub>2</sub> (PC 0.05M KOH)	>300	-	<i>Catal. Today</i> , 262 (2016) 170-180.

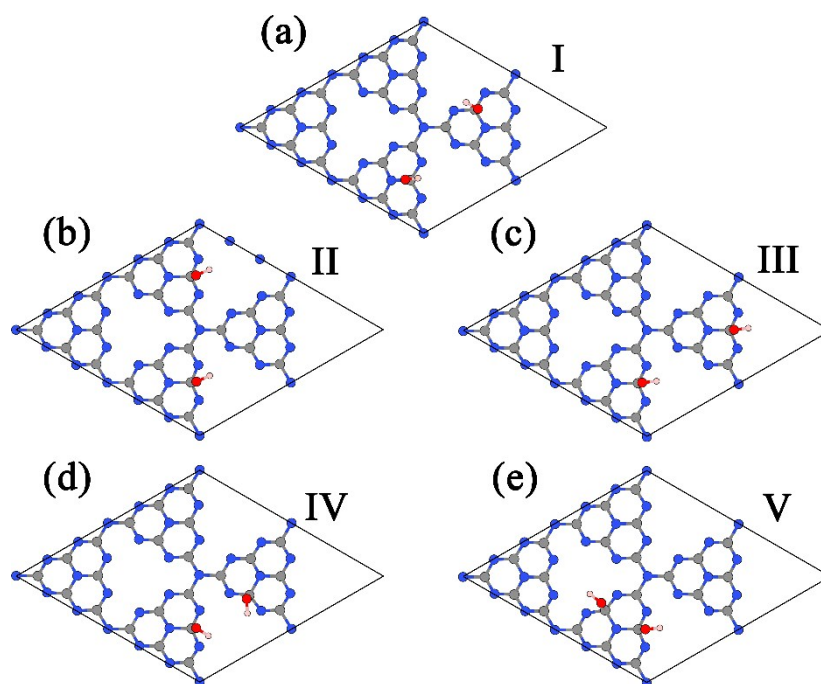


**Fig. S12.** The top view of five (a-e) different configuration of CN-s. The grey, blue, red and pink circles denote C, N, O and H atoms, respectively.

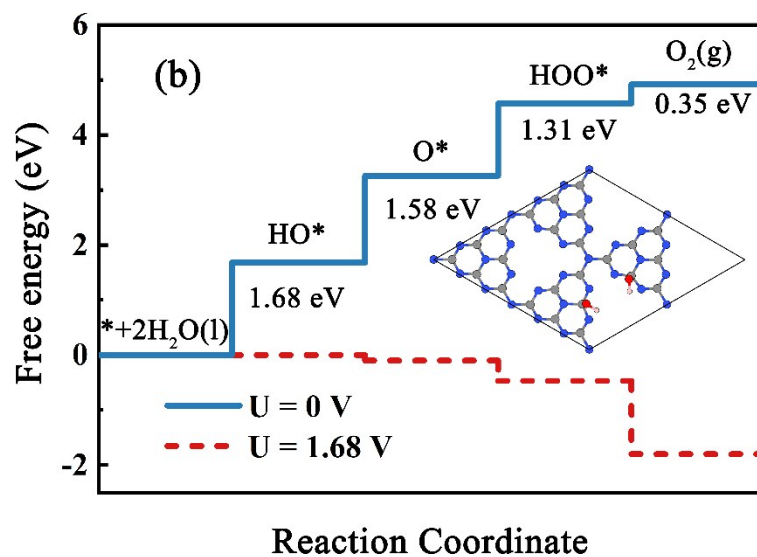


**Fig. S13.** Free energy diagram for the OER of CN-s with configuration III. The blue solid line and red imaginary line represent OER at zero potential ( $U=0$ ), and at the potential for which all steps become downwards, respectively.

**Table S5.** The energies of five different configuration of CN-s.

Configuration	Energy (eV)
I	-492.46
II	-492.26
III	-492.20
IV	-492.32
V	-492.01

**Table S6.** The adsorption energies (eV) of intermediates OH, O and OOH.

System	OH	O	OOH
CN	-1.80	-3.51	-0.43
CN-s	-1.82	-3.78	-0.61

**Table S7.** Comparison of H<sub>2</sub> evolution activities of CN-s-1.5 photocatalyst with other CN-based photocatalysts under visible light irradiation.

Photocatalyst	sacrificial	Light source	Pt cocatalysts dosage (%)	H <sub>2</sub> evolution activities (μmol h <sup>-1</sup> g <sup>-1</sup> )	Ref.
CN-s-1.5	Methyl alcohol (10 vol%)	300W, Xe lamp (λ>420 nm)	1%	124.6	This work
N doped CN	TEOA (10 vol%)	300W, Xe lamp (λ>420 nm)	0.5%	70.7	20
N-vacant/g-C <sub>3</sub> N <sub>4</sub>	TEOA (10 vol%)	300W, Xe lamp (λ>400 nm)	3%	123	21
C, N-TiO <sub>2</sub> /g-C <sub>3</sub> N <sub>4</sub>	TEOA (10 vol%)	300W, Xe lamp (λ>400 nm)	0%	39.18	22
Ag <sub>2</sub> O/g-C <sub>3</sub> N <sub>4</sub>	TEOA (10 vol%)	300W, Xe lamp (λ>420 nm)	0%	32.88	23
MgFe <sub>2</sub> O <sub>4</sub> /g-C <sub>3</sub> N <sub>4</sub>	TEOA (10 vol%)	300W, Xe lamp (λ>430 nm)	1%	30.09	24
CdS/Au/g-C <sub>3</sub> N <sub>4</sub>	Methanol (20%)	300W, Xe lamp (λ>420 nm)	1%	19.02	25
CM1B <sub>x</sub> -C <sub>3</sub> N <sub>4</sub>	TEOA (10 vol%)	350W Xe lamp (λ>420 nm)	0.8%	118	26
CN nanosheets	TEOA (10 vol%)	300W Xe lamp (λ>440 nm)	6%	139	27
CN nanosheets	TEOA (10 vol%)	300W Xe lamp (λ>440 nm)	6%	157.9	28

## References

1. P. Liu, X. Gu, H. Zhang, J. Cheng, J. Song and H. Su, *Appl. Catal. B-Environ.*, 2017, **204**, 497-504.
2. E. Parzinger, E. Mitterreiter, M. Stelzer, F. Kreupl, J. W. Ager, III, A. W. Holleitner and U. Wurstbauer, *Appl. Mater. Today*, 2017, **8**, 132-140.
3. S. Grimme, J. Antony, S. Ehrlich and H. Krieg, *J. Chem. Phys.*, 2010, **132**, 154104.
4. S. Grimme, S. Ehrlich and L. Goerigk, *J. Comput. Chem.*, 2011, **32**, 1456-1465.
5. J. P. Perdew, K. Burke and M. Ernzerhof, *Phys. Rev. Lett.*, 1996, **77**, 3865-3868.
6. W. Yue and J. P. Perdew, *Phys. Rev. B*, 1991, **44**, 13298-13307.
7. B. Zhu, L. Zhang, B. Cheng and J. Yu, *Appl. Catal. B-Environ.*, 2018, **224**, 983-999.
8. Y. Zheng, Y. Jiao, Y. Zhu, Q. Cai, A. Vasileff, L. H. Li, Y. Han, Y. Chen and S.-Z. Qiao, *J. Am. Chem. Soc.*, 2017, **139**, 3336-3339.
9. I. C. Man, H.-Y. Su, F. Calle-Vallejo, H. A. Hansen, J. I. Martinez, N. G. Inoglu, J. Kitchin, T. F. Jaramillo, J. K. Norskov and J. Rossmeisl, *Chemcatchem*, 2011, **3**, 1159-1165.
10. J. K. Norskov, J. Rossmeisl, A. Logadottir, L. Lindqvist, J. R. Kitchin, T. Bligaard and H. Jonsson, *J. Phys. Chem. B*, 2004, **108**, 17886-17892.
11. K. Li, Z. Zeng, L. Yana, S. Luo, X. Luo, M. Huo and Y. Guo, *Appl. Catal. B-Environ.*, 2015, **165**, 428-437.
12. M. Shalom, S. Inal, C. Fettkenhauer, D. Neher and M. Antonietti, *J. Am. Chem. Soc.*, 2013, **135**, 7118-7121.
13. S. Guo, Z. Deng, M. Li, B. Jiang, C. Tian, Q. Pan and H. Fu, *Angew. Chem.*, 2015, **128**, 1862-1866.
14. C. Liu, H. Huang, L. Ye, S. Yu, N. Tian, X. Du, T. Zhang and Y. Zhang, *Nano Energy*, 2017, **41**, 738-748.
15. Q. Fan, J. Liu, Y. Yu, S. Zuo and B. Li, *Appl. Surf. Sci.*, 2017, **391**, 360-368.
16. Z. Huang, F.-W. Yan and G.-q. Yuan, *ACS Sustain. Chem. Eng.*, 2018, **6**, 3187-3195.
17. C. Liu, X. Dong, Y. Hao, X. Wang, H. Ma and X. Zhang, *New J. Chem.*, 2017, **41**, 11872-11880.
18. L. Li, Y. Zhao, M. Antonietti and M. Shalom, *Small*, 2016, **12**, 6090-6097.
19. Z.-F. Huang, J. Song, L. Pan, Z. Wang, X. Zhang, J.-J. Zou, W. Mi, X. Zhang and L. Wang, *Nano Energy*, 2015, **12**, 646-656.
20. Q. Li, B. Yue, H. Iwai, T. Kako and J. Ye, *J. Phys. Chem. C*, 2010, **114**, 4100-4105.
21. P. Niu, G. Liu and H.-M. Cheng, *J. Phys. Chem. C*, 2012, **116**, 11013-11018.
22. W. Chen, T.-Y. Liu, T. Huang, X.-H. Liu, G.-R. Duan, X.-J. Yang and S.-M. Chen, *RCS Adv.*, 2015, **5**, 101214-101220.
23. M. Wu, J.-M. Yan, X.-W. Zhang, M. Zhao and Q. Jiang, *J. Mater. Chem. A*, 2015, **3**, 15710-15714.
24. J. Chen, D. Zhao, Z. Diao, M. Wang, L. Guo and S. Shen, *ACS Appl. Mater. Inter.*, 2015, **7**, 18843-18848.
25. X. Ding, Y. Li, J. Zhao, Y. Zhu, Y. Li, W. Deng and C. Wang, *APL Mater.*, 2015, **3**, 104410.
26. M. Shalom, M. Guttentag, C. Fettkenhauer, S. Inal, D. Neher, A. Llobet and M. Antonietti, *Chem. Mater.*, 2014, **26**, 5812-5818.

27. Y. Kang, Y. Yang, L. C. Yin, X. Kang, L. Wang, G. Liu and H. M. Cheng, *Adv. Mater.*, 2016, **28**, 6471-6477.
28. Y. Kang, Y. Yang, L.-C. Yin, X. Kang, G. Liu and H.-M. Cheng, *Adv. Mater.*, 2015, **27**, 4572-4577.